https://ntrs.nasa.gov/search.jsp?R=19700016166 2020-03-12T03:06:58+00:00Z

N70-25471
CR-109618
70-19240

Gulf General Atomic
Incorporated

GA-10061

RADIATION EFFECTS IN SILICON SOLAR CELLS

QUARTERLY REPORT

by

B. C. Passenheim, R. A. Berger, J. F. Colwell,
R. E. Leadon, and J. A. Naber

Prepared under
Contract 952387
California Institute of Technology
Jet Propulsion Laboratory
4800 Oak Grove Drive
Pasadena, California 91103

CASE FILE
COPY

April 10, 1970

Gulf General Atomic
Incorporated
P.O. Box 608, San Diego, California 92112

GA-10061

RADIATION EFFECTS IN SILICON SOLAR CELLS

QUARTERLY REPORT

by

B. C. Passenheim, R. A. Berger, J. F. Colwell,
R. E. Leadon, and J. A. Naber

Prepared for
California Institute of Technology
Jet Propulsion Laboratory
4800 Oak Grove Drive
Pasadena, California 91103

CONTRACT 952387

This work was performed for the Jet Propulsion Laboratory, California Institute of Technology, as sponsored by the National Aeronautics and Space Administration under Contract NAS7-100

Gulf General Atomic Project 6105 April 10, 1970

CONTENTS

1. INTRODUCTION 1

2. TECHNICAL DISCUSSION 1
   2.1 Resistivity and Minority-Carrier Lifetime Measurements 1
   2.2 Electron-Spin Resonance Measurements 3
   2.3 Optical Absorption Measurements 4

3. USE OF COMPUTER PN CODE FOR PREDICTING PERFORMANCE OF SOLAR CELLS 5
   3.1 Description of PN Code 7
   3.2 Proposed Program for Predicting Solar Cell Performance 10

4. PLANS FOR THE NEXT REPORTING PERIOD 14

5. NEW TECHNOLOGY 14

REFERENCES 15

FIGURES

1. Experimental and computer output characteristics of N/P silicon solar cell 12

TABLES

1. Parameters Used in Model of N on P Solar Cell 13
2. Values of Current and Voltages for the Various Curves . . 13

1. INTRODUCTION

The overall purpose of this program is to ascertain the nature of the defects responsible for the degradation in output of silicon devices (solar cells) irradiated by space radiation. When the nature of the defects and their annealing mechanisms are known, it will be possible (1) to determine the parameters that will lead to development of radiation-hardened devices, (2) to predict the effects of radiation and annealing on solar cells, and (3) to make use of computer programs to predict radiation effects in solar cells on extended space flights.

The present effort is concentrated on the study of the effects of lithium on the production and annealing of damage in silicon. This work is being performed on lithium-diffused bulk silicon using measurements such as minority-carrier lifetime, electron-spin resonance (ESR), electrical conductivity, and infrared absorption. The temperature range from 77.5° to $400^{\circ}K$ is under investigation. The damage is introduced by 30-MeV electrons and fission neutrons.

During the first quarter of this contract year, effort has been concentrated on sample preparation, equipment modification, necessary preirradiation measurements, and analytical studies of solar cells.

2. TECHNICAL DISCUSSION

2.1 RESISTIVITY AND MINORITY-CARRIER LIFETIME MEASUREMENTS

During this reporting period, an ingot of high-purity Czochralski-grown quartz-crucible (QC) phosphorus-doped silicon was purchased from Wacker Chemical Company. Preliminary measurements indicate the resistivity of this ingot is approximately 90 ohm-cm and that its minority-carrier lifetime at room temperature is 100 μsec. The effect of heat

treatment on the resistivity of this material was investigated because Fuller and Logan[1] report observing a substantial increase in donor density in quartz-crucible silicon heated to 450°C in an inert atmosphere. Since lithium is diffused into bulk silicon at 400° to 450°C, such a heat-treatment effect would complicate any estimate of lithium density based on resistivity measurements after diffusion.

Preliminary measurements on the effect of a 450°C heat treatment on slices of silicon taken from this ingot indicate the donor density increase is less than 10^{13} $(cm^3\text{-}hr)^{-1}$. Fortunately, this rate is much less than the donor density increase due to the lithium diffusion and the redistribution cycle, and may prove to be negligible.

The possible effect of heat treatment on minority-carrier lifetime was also investigated. Adjacent slices of silicon were cut from the ingot. One was diffused by the lithium-oil paint-on technique, the other was subjected to an identical temperature cycling. After heat treatment, the resistivity of the diffused sample was 0.35 ±0.05 ohm-cm compared to 65 ±5 ohm-cm for the nondiffused slice. The minority-carrier lifetime at 300°K of the nondiffused slice was still 100 μsec, while the lifetime of the diffused slice was 30 μsec; indicating temperature cycling during sample preparation has negligible effect on the preirradiation lifetime.

Conventional four-lead minority-carrier lifetime samples have been fabricated from lithium-diffused bulk QC silicon. Control samples of nondiffused silicon, subjected to identical heat treatments, were also fabricated. The preirradiation temperature dependence of minority-carrier lifetime is being measured for both diffused and control samples, to separate the recombination center due to lithium diffusion from the recombination centers initially present.

An effort to develop a computer subroutine to reduce minority-carrier lifetime and conductivity experimental data was initiated during the first quarter, but has not been completed.

The study of the degradation and anneal of minority-carrier lifetime of electron-irradiated lithium-diffused float-zone silicon was continued during this quarter. Two 30-MeV electron irradiations were performed at Linac. This data will be presented as soon as it is completely reduced.

2.2 ELECTRON-SPIN RESONANCE MEASUREMENTS

The electron-spin resonance of the phosphorus-vacancy (Si-G8) center has continued. Our previous study indicated that lithium diffusion reduced the initial number of paramagnetic phosphorus donors and that the Si-G8 introduction rate was reduced in electron-irradiated lithium-diffused phosphorus-doped silicon.

These results suggest two questions. Since it is known that when lithium is diffused into silicon containing oxygen, a lithium oxygen (LiO) complex is formed, does the reduction of the paramagnetic phosphorus density imply the formation of a lithium phosphorus (LiP) complex? Furthermore, since the introduction rate of phosphorus-vacancy (Si-G8) defects is reduced in lithium-diffused silicon, where does the mobile radiation-induced vacancy go? That is, does the free lithium compete with the phosphorus for the vacancies, and if a lithium-phosphorus complex is formed, does it interact with radiation-induced vacancies?

In our previous investigation, samples had densities of approximately 1.1×10^{16} cm^{-3} phosphorus and 3.6×10^{16} cm^{-3} lithium. Samples currently being investigated have approximately 1×10^{16} cm^{-3} lithium and 1×10^{16} cm^{-3} phosphorus. By varying the lithium-to-phosphorus ratio, we hope to determine whether lithium-phosphorus complexes are formed during lithium diffusion. By measuring the irradiation-produced defect center introduction rates for various impurity concentrations, we hope to obtain information on the relative capture cross sections of the impurities.

This investigation was resumed with a 77°K irradiation of carefully oriented lithium-diffused phosphorus-doped silicon samples to 30-MeV electron fluences of about 6×10^{16}, 8×10^{16}, and 1×10^{17} e/cm^2. ESR measurements of these samples, and of diffused and non-diffused control samples which have not been irradiated, are currently in progress.

In our previous search for the Si-G8 center, an unidentified center with $1.982 \leq g \leq 1.997$ was observed. The impurity dependence of the introduction rate of this center is also being investigated in an effort to establish its identity.

2.3 OPTICAL ABSORPTION MEASUREMENTS

Both ESR and optical absorption techniques were used in our previous investigation of the divacancy in electron-irradiated lithium-diffused float-zone silicon. No divacancies were observed in samples irradiated at 77°K or 300°K with 30-MeV electrons. From ESR measurements, it was concluded that either (1) the introduction rate of divacancies was greatly reduced by the presence of lithium or (2) the divacancy introduction cannot be determined because the divacancy was in a nonparamagnetic charge state. Optical absorption measurements, which do not depend on the divacancy's charge state, were made on the most heavily irradiated ESR samples, and no divacancies were detected. However, this sample had been warmed to room temperature during the ESR investigation, so that it was possible that annealing by lithium motion had occurred. During this quarter, samples of diffused and nondiffused high-purity float-zone silicon have been prepared specifically for optical measurements. These samples were all made from 10^4 ohm-cm phosphorus-doped float-zone silicon. They are all approximately 2mm x 5mm x 10mm, with the 5mm x 10mm faces polished to a mirror-like finish with one micron diamond paste. The lithium-diffused samples were diffused by the paint-on technique to an estimated lithium density of 5×10^{16} cm^{-3} ($\rho = 0.15$ ohm-cm) before polishing. These samples were

irradiated with the ESR samples to a fluence of about 10^{17} e/cm^2 (30 MeV) at 77°K, and are being maintained at 77°K until they can be irradiated to a total fluence of about 3×10^{17} e/cm^2. From this study, we expect to determine the actual divacancy introduction at 77°K. Since these samples will not have been warmed above 77°K, annealing experiments are also possible.

3. USE OF COMPUTER PN CODE FOR PREDICTING PERFORMANCE OF SOLAR CELLS

Although the work under this contract is being done on bulk silicon diffused with lithium, the desired ultimate goal is an operating device—namely, a solar cell—that is resistant to radiation damage. Therefore, in addition to measuring changes in the electronic properties of bulk materials due to damaging radiation and annealing, it is important to be able to predict the effect of such changes on the device performance. The conventional analyses of solar cell performance have usually taken two approaches. In the first, the short-circuit current of the solar cell is calculated based on diffusion theory, assuming uniform carrier lifetimes (or diffusion lengths) on the two sides of an estimated depletion region. The second approach consists of fitting experimental data to the solar cell equation to empirically determine the four unknown parameters in the equation.

While both of these methods can yield useful results for many purposes, they both have shortcomings for application to radiation damage studies. Although the first method attempts to relate performance to the bulk material properties of the device (for example, lifetimes, diffusion constants, generation rate of excess electron-hole pairs, etc.), it is usually necessary to assume that the parameters are constant on either side of the junction. Thus, it is difficult or impossible to correctly simulate the effects of non-uniform damage and the attenuation of the light intensity with depth into the device. Also, it is usually necessary to make other simplifying assumptions, for example, quasi-charge neutrality in the bulk of the

device, zero-carrier densities at the edge of the depletion region, and no recombination in the depletion region. Moreover, this method is strictly applicable only to short-circuit conditions, and attempts to predict performance as a function of load would require additional assumptions. On the other hand, the solar cell equation predicts the device performance versus load, but it is difficult to relate the empirically-determined parameters of the equation to the properties of the material, especially if the radiation damage is not uniformly distributed throughout the device. Thus, one needs a new method, one which predicts the output of a solar cell as a function of its exterior load, the basic material properties, and the distribution of damage.

Under government contracts, Gulf General Atomic Incorporated (GGA) has developed a computer code called PN[2] which is ideally suited for this problem. This code is currently operational and has already been used to investigate a number of problems involving transient ionization effects in electronic devices. With no modifications, it can be used to predict the steady-state I-V characteristics of solar cells with arbitrary doping profiles, spectral intensity of light, non-uniform radiation damage, etc. It can include also the degradation of carrier lifetimes with radiation fluence and the annealing of this damage with time. However, for most solar cell applications, the damage is introduced so slowly compared to the annealing rate that steady-state damage constants can be used. An earlier version of the code is described in detail in Ref. 2 but some additional features that are useful for simulation of solar cells have been added during the past year. The general features of the code that are of interest for solar cell problems are described briefly in Section 3.1. The planned program for demonstrating the usefulness of this code in predicting solar cell performance is outlined in Section 3.2.

3.1 DESCRIPTION OF PN CODE

The PN code is applicable to devices that can be approximated in one dimension, either linear in rectangular geometries or radial in cylindrically symmetric or spherically symmetric geometries. In the following, the discussion will be confined to the linear geometry.

The basic equations that are solved by the computer for the interior of the device are the one-dimensional continuity equations for the two charge carriers, n and p,

$$\frac{\partial n}{\partial t} = g - R - \frac{\partial J_n}{\partial x}$$

$$\frac{\partial p}{\partial t} = g - R - \frac{\partial J_p}{\partial x}$$

and Poisson's equation for the electric field E,

$$\frac{\partial E}{\partial x} = \frac{4\pi q}{\kappa} [p - n + \Delta N] \quad .$$

In these equations, n is the density of electrons in the conduction band, p is the density of holes in the valence band, ΔN is the net density of doping of the semiconductor (positive for donors, negative for acceptors), q is the magnitude of the electronic charge, and κ is the dielectric constant. The term g is the generation rate of electron-hole pairs due to the incident radiation, and R is the rate of recombination of excess electrons and holes. Usually, the recombination rate is simulated by a Shockley-Read[3] type equation of the form

$$R = \frac{np - n_o^2}{\tau_{n_o} (p + p_F) + \tau_{p_o} (n + n_F)} \quad ,$$

where n_o is the intrinsic carrier density, n_F and p_F are the values of n and p when the Fermi level coincides with the energy level of the recombination center, and τ_{n_o} and τ_{p_o} are the low-injection-level recombination lifetime of electrons in heavily p-type material and of holes in heavily n-type material, respectively. However, if desired, more complicated types of recombination, including trapping, are available. For radiation damage and annealing, τ_{n_o} and τ_{p_o} change with fluence and time. The quantities J_n and J_p are the particle current densities given by

$$J_n = -n\mu_n E - D_n \frac{\partial n}{\partial x} = nv_n - D_n \frac{\partial n}{\partial x} ,$$

$$J_p = p\mu_p E - D_p \frac{\partial p}{\partial x} = nv_p - D_p \frac{\partial p}{\partial x} .$$

The E (or velocity v) terms are the drift currents with mobilities μ_n and μ_p, and the $\partial/\partial x$ terms are the diffusion currents with diffusion coefficients D_n and D_p. Temperature enters the problem by Einstein's relation between the μ's and the D's and in the values of n_o, μ_n, μ_p, τ_{n_o}, τ_{p_o}, n_F, and p_F. In these equations, n, p, g, τ_{n_o}, τ_{p_o}, and E can be functions of time and position while ΔN, μ_n, and μ_p are constant in time but are functions of position.

The device is connected to an exterior circuit that can include various arrangements of batteries, resistances, capacitances, and inductances. However, for solar cell applications the exterior circuit will normally consist of a single exterior resistance connecting the two ends of the device. The code calculates the current in the exterior circuit by summing voltages around the loop, including internal electric fields inside the device and contact potentials at the two contacts, and dividing by the exterior resistance. The boundary conditions require that the exterior current equals the internal current inside each end of the device.

Several types of boundary conditions at the contacts are available. One, called "bulk" conditions, forces the slope of the carrier densities to be zero at the boundaries. This condition is suitable if the details of the boundaries are not important and carrier densities can be assumed to have their bulk values, that is, their values, far from any discontinuity in the device. However, if differences in the work functions of the semiconductor and contacrs are important, the "bulk" contact potentials, which are automatically included in the code as a function of doping to give the proper summation of voltages around the circuit, can be modified to account for the difference in work functions. Finally, if ohmic contacts are desired, a thin region of high recombination rate can be simulated at each contact.

To solve the time-dependent partial differential equations, they are converted into finite difference forms, and the resulting algebraic equations are solved by iteration for finite-time step intervals. The details of the differencing and iteration procedures are described fully in Ref. 2 and will not be repeated here. Suffice to say, the transient and steady-state solutions obtained from the code give excellent checks with problems that can be solved analytically. The mesh distribution for the finite differences is arbitrary, but the permissible total is limited to 300 stations by the capacity of the Univac 1108 computer. This number is quite adequate for simulating a solar cell. The mesh spacing can be made small where the variables are changing rapidly with position, such as near junctions, and they can be spaced further apart where the variables are changing more slowly. The code has an automatic remesh feature in case the densities change more rapidly than a specified ratio between adjacent mesh stations.

To start a new problem, the code starts from an arbitrary but mathematically consistant set of distributions of densities and electric fields. This initial distribution is usually physically unrealistic, but the code then proceeds in time to the correct physical

situation depending on the input parameters. If one then desires to make a small change to the system, such as changing the exterior resistance, it is usually permissible to start from the end of the previous run and make the change, rather than starting over from the arbitrary initial distribution.

The advantages of this code over most other methods of analysis are (1) it is not necessary to make arbitrary assumptions about the boundary conditions at the edge of the depletion region or about quasi-charge neutrality in various regions of the sample, (2) recombination inside the depletion region can be considered, and (3) the doping profile and the distributions of recombination centers and carrier generation rate inside the sample can be simulated to any reasonable degree of complexity. Thus, the user has the assurance that what he obtains from the computer is not a byproduct of some dubious assumption that he may have had to make in order to obtain a solution but is the rigorously correct solution for the equations of the system, within the accuracy of the finite difference approximations.

3.2 PROPOSED PROGRAM FOR PREDICTING SOLAR CELL PERFORMANCE

The purpose of this program is to demonstrate that the PN code can generate realistic performance curves for solar cells and can reasonably predict the effect of various parametric changes which are hard to analyze by other methods. Consequently, this work will not be directed toward any specific device, but whatever experimental data that are available and pertinent will be used for comparison.

At the start, the code will be applied to typical, undamaged solar cells, and the predicted I-V curves will be compared to experimental data, such as in Ref. 4. The effect of the type of incident light (different attenuation of electron-hole generation rate with depth) can be studied as well as the effect of light intensity and changes in the device parameters, such as doping profiles, carrier

lifetimes, etc. Once a reasonable representation of the undamaged solar cell has been obtained, non-uniform damage due to low-energy protons will be simulated. The depth and distribution of the damage will be estimated from Ref. 5 and the changes in the predicted I-V curves will be compared to the available experimental results, such as Lodi.[4]

Some initial results from the computer are plotted in Fig. 1a, along with two typical experimental curves (Fig. 1b) from Refs. 4 and 6. For convenience of comparison, all curves have been normalized to the short-circuit currents and open-circuit voltages. The two theoretical curves are based on an assumed, realistic doping profile and lifetime characteristics. One curve (labeled Run 104) is for a uniform generation rate throughout the sample of 10^{21} cm^{-3}/sec corresponding to sunlight at the surface of the cell with an arbitrary reflection and coverslip loss of 0.08. The other has this same generation rate at the illuminated surface, but it is attenuated with depth. The attenuation is calculated from the absorption coefficient for silicon quoted by Kleinman.[7] The two experimental curves are for devices whose basic parameters are not definitely known, so they should not be compared in detail with the theoretical curves. They are presented only to illustrate the general similarity of results. However, the nominal characteristics of the TI cell were estimated (Table 1), and these were used in the calculations. In the future, an attempt will be made to obtain better estimates of the parameters for the experimental cells so that comparison of theoretical and experimental results will be more meaningful. Table 2 lists the open-circuit voltages and short-circuit currents for the curves in Fig. 1b. The values for run 300 are about one-half of the TI cell measured results. This may indicate that the doping level and lifetime in the N region should have been about twice the values given in Table 1.

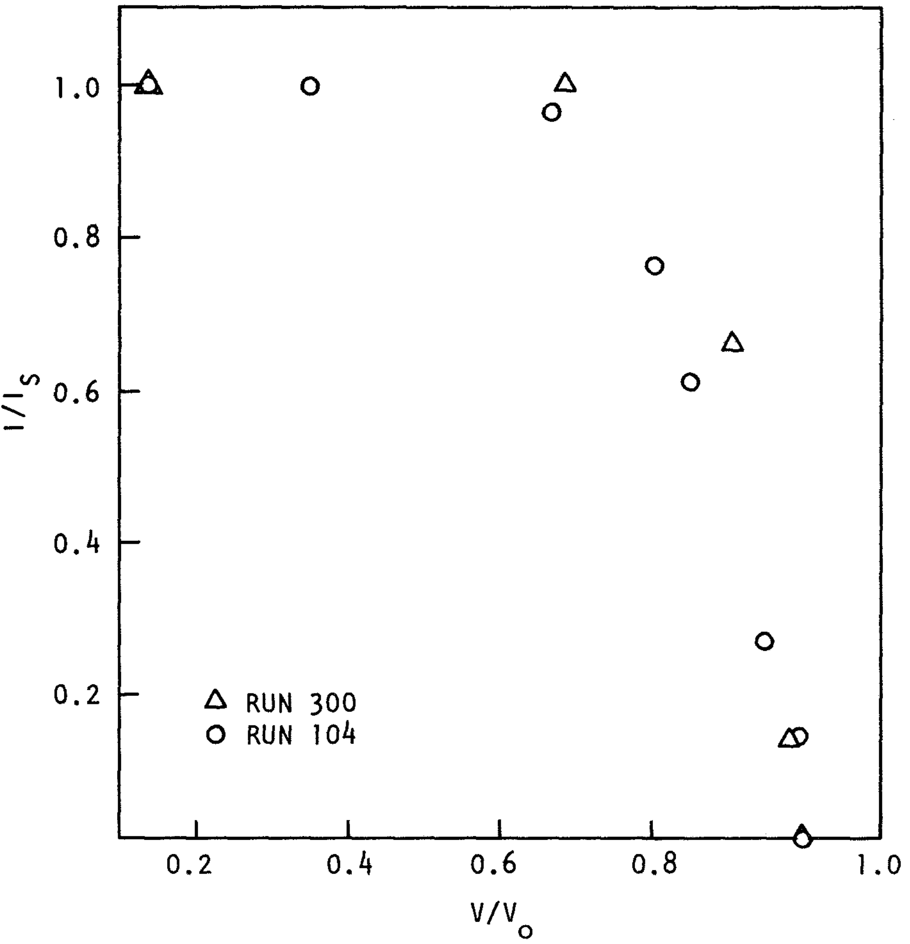

(a) CALCULATED CURVES

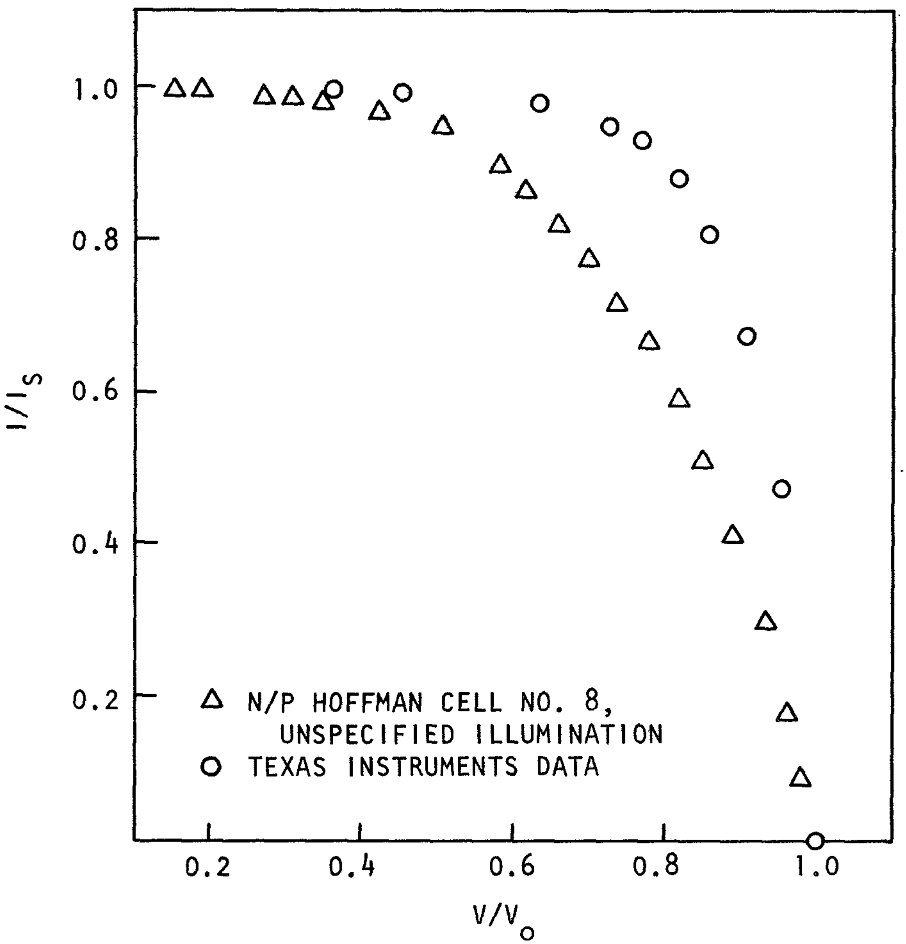

(b) EXPERIMENTAL CURVES

Fig. 1. Experimental and computer calculative output characteristics of N/P silicon solar cell

Table 1

PARAMETERS USED IN MODEL OF N ON P SOLAR CELL

	Doping (cm^{-3})	Lifetime (msec)		Mobilities (cm^2/nsec)	
		electrons	holes	electrons	holes
N Region	3.0×10^{17}	0.01	1.0	670.0	220.0
P Region	1.5×10^{15}	5.0	0.1	1230.0	430.0

Cross section area: 1 cm^2, depth of junction: 10^{-4} cm, total length: 3.8×10^{-2} cm.

Table 2

VALUES OF CURRENT AND VOLTAGES FOR THE VARIOUS CURVES

	TI	LODI	Run 300	Run 104
Open-circuit voltage	0.55	0.52	0.241	0.302
Short-circuit current (amps)	2.9×10^{-2}*	3.4×10^{-2}	4.42+	

*Normalized to an area of 1 cm^2.

+This run, in which the light intensity was uniform, had a generation rate in the bulk region some 2 or 3 orders of magnitude larger than the generation rate for Run 104.

4. PLANS FOR THE NEXT REPORTING PERIOD

In the next reporting period, we expect to complete the irradiation of samples to be used in the optical absorption measurements. These samples and ESR samples will be irradiated simultaneously at liquid nitrogen temperatures with 30-MeV electrons and maintained at 77°K, in an effort to prevent defect annealing as a result of lithium diffusion, until examined.

ESR, optical absorption, and minority-carrier lifetime studies of electron-irradiated lithium-diffused silicon will be continued during the next reporting period.

The computer determination of solar cell output will continue.

5. NEW TECHNOLOGY

No new technology is currently being developed or employed in this program.

REFERENCES

1. C. S. Fuller and R. A. Logan, J. Appl. Phys. 28, 1427 (1957).

2. R. E. Leadon and M. Vaughn, "Short-Pulsed Radiation Effects on Dynamic Electronic Components," Final Report, Contract DASA01-68-C-0123, 5 June 1969, Report No. DASA 2358 or GA-9397.

3. W. Shockley and W. T. Read, Phys. Rev. 87, 835 (1952).

4. Edward Lodi, Vol. 1, Photovoltaic Specialists Conference p. B-4-1 (1963).

5. Yu. V. Bulgakov and T. I. Kolomenskaya, Soviet-Physics-Semiconductors, 1, 346 (1967).

6. Texas Instruments Bulletin No. DL-S 657985, August 1965 (10-Ω-cm base material).

7. D. A. Kleinman, B.S.T.J. 40, p. 85 (1961).